Ultracompact gas-sensor based on a 2D photonic crystal waveguide incorporating with tapered microcavity

Ultracompact gas-sensor based on a 2D photonic crystal waveguide incorporating with tapered microcavity

A Harhouz[1], A Hocini[1,*] and H Tayoub[1,2]

[1]Laboratoire d'Analyse des Signaux et Systèmes, Department of Electronics, University of M'Sila BP.166, Route Ichebilia, M'Sila, 28000, Algeria.
[2]Research Center in Industrial Technologies CRTI, P.O.BOX :64, Cheraga 16014, Algiers, Algeria

*E-mail: abdesselam.hocini@univ-msila.dz

Abstract. In this study, a new ultra compact gas-sensor, based on a 2D photonic crystal waveguide incorporating with tapered microcavity, is designed to detect small refractive index changes. The refractive index (RI) sensor is formed by a point-defect resonant cavity in the sandwiched waveguide on Si slab with triangular lattice. The properties of the sensor are simulated by using the plane wave expansion (PWE) method and the finite-difference time-domain (FDTD) algorithm. The transmission spectra of the sensor with different ambient refractive indices ranging from n = 1.0 to n = 1.01 are calculated. The calculation results show that a change in ambient refractive index of $\Delta n=1\times10^{-4}$is apparent. The proposed sensor achieves a sensitivity ($\Delta\lambda/\Delta n$) of 523.2 nm/RIU. It was found that the resonance wavelength is a linear function of the refractive index in under study range. The sensor is appropriate for detecting homogeneous media.

1. Introduction

Photonic crystal (PC) sensors attracted attention of many researches due to the locally confined optical state into tiny volume [1, 2]. One among the types of optical sensors are refractive index-based sensors whose application has become widely covering many functions, for instance, measurement of parameters such as humidity [3], temperature [4], gas [5, 6], chemical composition|, and biosensing. The refractive index (RI) biosensors have received substantial attention in the development of label-free biomedical and biochemical measure. Accordingly, the target analytes can be sensed in their natural forms with no need of any adjustments [7-9]. Besides, RI change is directly associated with the concentration of liquids or gases, or their existence rather than the entire sample volume, therefore, sensitive free-label detection with small sample volumes can be realized by the RI sensor.

Photonic crystal is a periodic dielectric structure with the potential of directing and manipulating light at the optical wavelength scale [10]. Specifically, the periodic air hole microstructure of hole-type PC is a natural candidate for housing target liquids or gases. PCs are appealing sensing platforms since they provide strong light confinement. Unlike many platforms that use the interaction between the small evanescent tail of of the electromagnetic field and the analyte, PCs can be designed to localize the electric field in the low RI region which makes the biosensors extremely sensitive to a small RI change produced by infiltrated analytes on the air holes [11].

The quality factor Q of wavelength-sized microcavities in two dimensional (2D) photonic crystal slab structures [12, 13] was formerly considered as being limited by vertical radiation loss. Yet, a pletora of studies have indicated that these structures can achieve a high Q value [14, 15] in case of using a proper design intended to decrease the perpendicular radiation. The PCs heterostructure concept is used, a line-defect structure whose width is locally adjusted, to achieve high and ultrahigh quality-factor cavities [16].

This study puts forward a novel ultra-compact gas-sensor based on new design for the microcavities in a PCs;namely, a line-defect structure whose width is locally adjusted. The mode gap, existing in the waveguide, results in the confinement found in the direction of a line defect. The mode gap's location can be changed by changing the geometrical parameters of line-defect waveguides [17-19], this enables the creation of a local confinement potential within theoretically lossless waveguides. The properties of the sensor are simulated using the plane wave expansion (PWE) method and the finite-difference time-domain (FDTD) algorithm (RSoft Photonic Suite).

2. Structure design

First, a precise geometry of 2D photonic crystal Si slab infiltration is proposed, specifically, targeting the waveguide where most of the mode energy exists as an optical detector.

We consider a 2D PC slab with a triangular array of air holes (n_{air}= 1) in a silicon slab (n_{si}= 3.42) with h=230 nm of thickness, as illustrated in figure 1, making use of the triangular PCs is practically important due to their large transverse electric band gap, which is expected to serve as a good platform for photonic integrated circuits and ultra-compact optical sensors [20].The structure has holes of radius=140 nm with lattice constant a=430 nm.

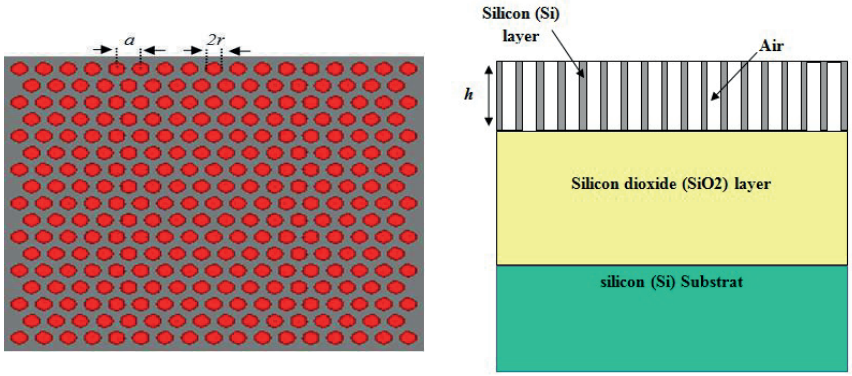

Figure 1. The host structure of PC, 2D triangular lattices, consisting of air holes with a lattice constant of a=430 nm, air hole radius r, is equal to 140 nm and size of photonic crystal is 23×23.

To support the Si Slab, Silicon dioxide (SiO_2) layer with a thickness of 1500 nm is used as a base. The low index of SiO2 layer located underneath the high index of Si slab enables to confine light within the cavity core, hence, avoiding optical losses into the lower substrate. Consequently, the light confinement in the vertical direction is ensured by total internal reflection.

In 3D-FDTD calculation, CPU time and a large computer memory are requisite. Meantime, 2D-FDTD calculation using effective RI approximation method notably cuts down both the computer memory and the simulation times, leading to a reasonable estimation. In 2D-FDTD method, the vertical confinement achieved in z direction is totally ignored; however, the magnitude of the loss in z direction is very low. To reduce the computational efforts required for the full 3D calculations, the PC is replaced by a 2D system with the background dielectric medium having the effective refractive

index of 2.838 that corresponds with the efficient index of the fundamental guided TM mode at wavelength of 1550 nm.

The following procedure was the calculation of a photonic bandgap for TM polarization, which ranges of1241.69nm to 1659.93 nm (figure2). It was calculated along the Γ-K-M-Γ edge for the Brillouin zone using a 2D plane wave expansion (PWE) method of the RSoft (BandSOLVE) software and the FDTD algorithm of the RSoft (full wave).

A PC slab waveguide can also be formed by removing one row of air holes in the ΓK direction. Light, which propagates in the waveguide with a frequency within the bandgap of the crystal, is confined too, and can be directed along the waveguide (figure 3).

During the simulation process, the light source was positioned in the input line defect waveguide head, as for the monitor, it was placed at the end of the output line waveguide. The normalized central frequency of Gauss pulse source is centered around 0.26(2πc/a). Since there must be a careful consideration of the boundary conditions at the spatial edges of the computational domain, one-spatial unit thick perfectly matched layer (PML) encircling the simulated area is set to absorb the fields enabling the simulated region to implement reflections.

The transmission spectrum of the PC waveguide, obtained by using of a 2D FDTD method, has shown in figure 4. For PC structures, the nature of waveguide modes depends on its location in the bandgap. One can observe that light with a frequency within the bandgap can propagate in the waveguide.

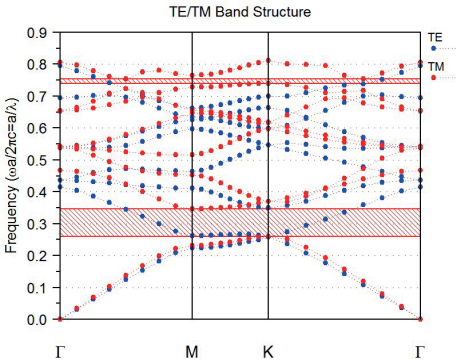

Figure 2. Photonic bandgap for TM polarization, using PWE method of the RSoft (BandSOLVE) software.

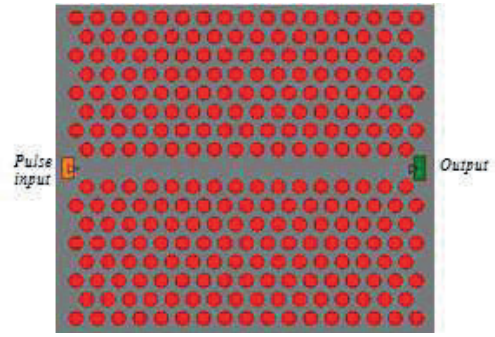

Figure 3. Schematic view of the proposed waveguide in Si slab.

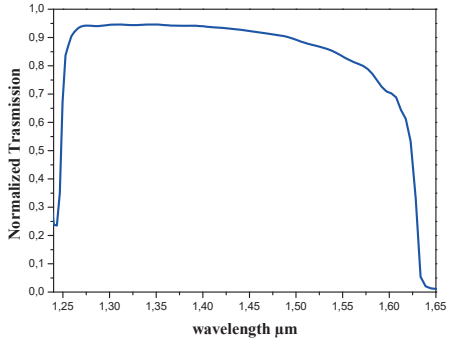

Figure 4. Transmission spectrum for the PC waveguide; using FDTD algorithm of the RSoft (full wave).

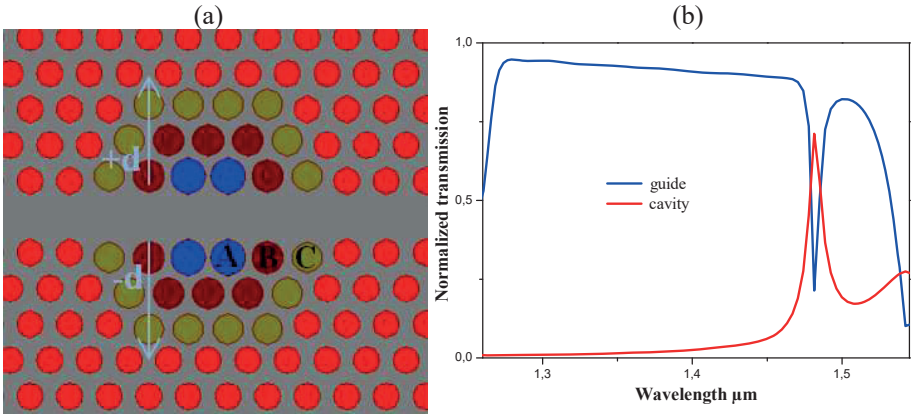

Figure 5. (a)The reference design of the proposed RI sensor.The hole's radiuses are: r_A=0.442a nm, r_B= 0.395a nmandr_C=0.372a.(b)The transmission spectra of the designed structure.

Sensors based on PC waveguides incorporating with microcavities hold numerous merits in compactness, high quality (Q) factor and sensitivity, easy extension to sensor arrays and various choices of materials, and in parallel measurement capacity [21-26]. Furthermore, a tapered-shift structure along the line defect increases the quality factor of the cavity [27]. Thus, the proposed RI sensor is created by means of two waveguide couplers and microcavity in the PC with a triangular lattice of air holes (see figure5).

The microcavity is designed by changing of the size of 30 air holes in the center of the line defect. The holes radiuses areas r_A=0.442anm, r_B =0.395anm an dr_C=0.372 anm. Another defect is realized by increasing the waveguide width at the center of the microcavity by moving the surrounding holes A, B, C away from the waveguide by a distance of -d, +d.

The FDTD method has been applied by the considered grid-size (Δx, Δz) of 43 nm when the lattice constant is 430 nm, so the resolution is set to 10 (that is, with a grid size of a/10, where a represents the lattice constant). A Gaussian exciter has been used with a central wavelength of 1.550µm. Pulsed light is launched from the left (arrow).The output is measured at the right (time monitor), and the time step of 0.035 a/c is employed. All the simulations are carried out with the same mesh size and time step for future equivalent results. The FDTD algorithm depends on structure meshing, accordingly, the prominent impact to be noticed is the dependence of the results on mesh size. Reducing the mesh size should bring the results to a given limit, however, reduction of mesh size can also reduce time step which can lead to deviations in the comparison of the results. In the X and Z directions, when the mesh is reduced from 43 to 21.5 nm (the half), the results remain almost constant indicating that the method has converged.

3. Simulation results and discussion

The sensing principle is based on the shift of resonance wavelength λ_0, which occurs due to the change in RI of the sensor when the PC's air holes are full of homogenous gas. The effective RI of the slab and the RI contrast between the holes and the slab region are changed, by varying the local RI. Since the transmitted wavelengths depend directly on the effective index of the slab [23], the device can be used as a sensor by detecting the output transmission spectrum. With the presence of gas, the effective RI changes and hence causes a shift in the cut-off wavelength or resonance wavelength λ_0 (waveguide or waveguide incorporating with micro-cavities) of the output spectrum. This phenomenon can be

analyzed by using the first-order electromagnetic perturbation theory. This latter is due to a small perturbation $\Delta\varepsilon \approx 2n\Delta n$ [28].

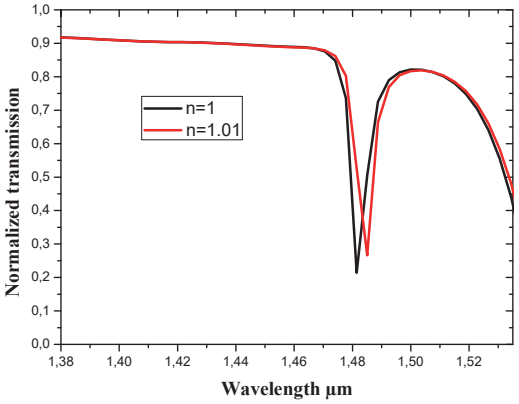

Figure 6. Calculated transmission spectra for TM polarization of the reference RI sensor.

The microcavity gives a shift of 3.667nm, equivalent to the sensitivity of 366.7 nm/RIU for a change in RI value of 0.01. (figure6). concerningRI measurements, the sensitivity (S) is calculated as the ratio of the resonance wavelength λ_0 shift and the change in the RI and its unit is given by nm/RIU. Thus, equation can be written as:

$S=\Delta \lambda_0/\Delta n$ (2)

where$\Delta n=n-n_0$ and $n_0=1$.

To improve the sensitivity of the sensor, we present a new design (figure7 (a)). It is necessary to highlight here that ring-shaped holes configuration does not only offer more flexibility, indesigning new structures compared to circular shaped ones, but also enhance the optical field confinement and, hence, the light-fluid (gas) interactions within the ringed low-dielectric material area[9,29,30].

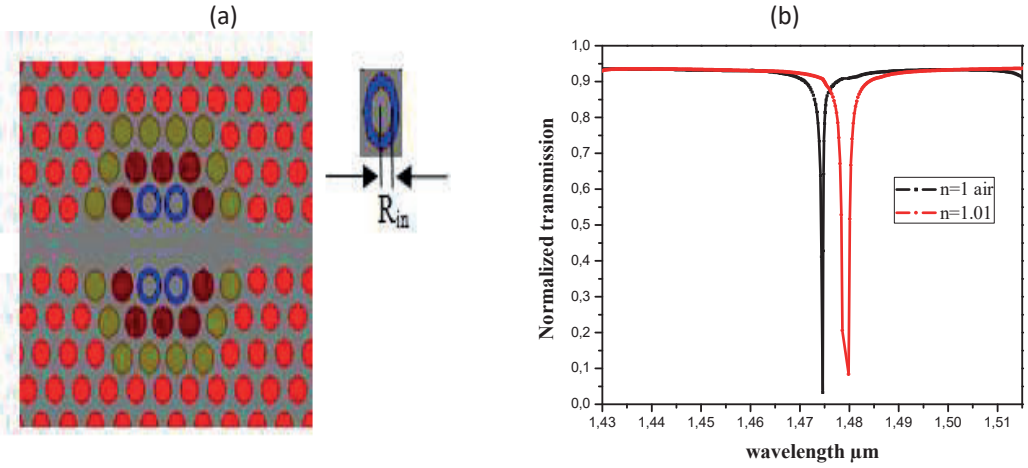

Figure 7. (a)The design of the proposed RI sensor. (b) The transmission spectra of the designed device for $R_{in}=0.325a$.

The optical free-label detection properties of the designed structure has been quantitatively estimated by the sensitivity parameter S ($\Delta\lambda/\Delta n$), which is defined as the ratio of shift in the wavelength ($\Delta\lambda_0$) to the change in the RI due to gas infiltration (Δn). According to the obtained results the output resonant wavelength is red-shifted due to the increase in the ambient RI of the sensing area

(figure 7 (b)), which confirms the gas identification. A change in the RI of Δn=0.01 results in a spectral red-shift of 5.225 nm which corresponds to a RI sensitivity of 522.5 nm/RIU.

(a) (b)

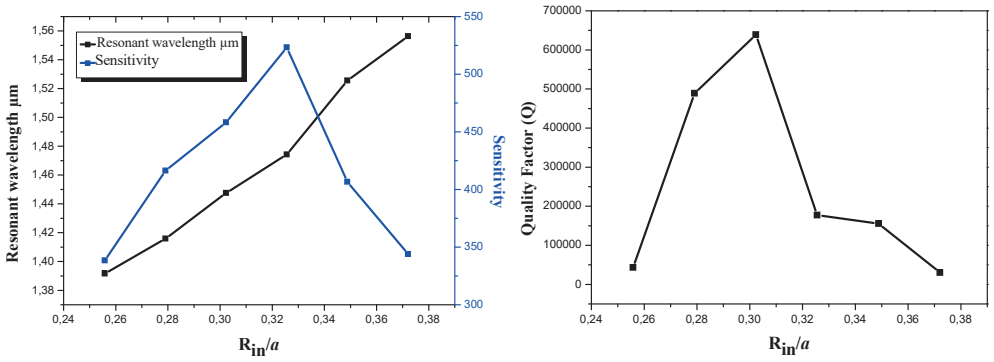

Figure 8.(a)The sensitivity and the resonant wavelength variations according to the change of the inner radius (R_{in}) from 0.255a to 0372a. (b) The quality factor Q as afunction of the inner radius change (R_{in}).

Table 1. Resonant wavelength (λ_0), sensitivity (S) as function of Refractive index (RI).

RI	λ_0 (µm)	*S (nm/RIU)*
1	1.474625	-----
1.000139	1.474700	539.56
1.00026	1.474750	480.76
1.00047	1.474870	521.27

The sensor, additionally, needs to have high transmission efficiency and high Q factor, which can increase the detection feasibility and make it easier. The transmission efficiency can be denoted asA_0/A_i, where A_0 is the output amplitude of magnetic-field at resonance peak, A_i is the input amplitude of magnetic-field at the same frequency. The Q factor is defined as ω_0/ω_x, where ω_x is the full width at half-maximum (FWHM) of the resonator's Lorentz a response, and ω_0, is the resonance frequency [38].

Table 2. Comparison of the proposed gas sensor with various PC designs.

References	Sensing structure	Sensitivity (nm/RIU)	Q factor	Detection limit (RIU)
[34]	Photonic crystal waveguide utilizing width modulated microcavity	80	40 000	10^{-4}
[35]	Photonic crystal microcavity	433	3000	10^{-4}
[36]	Air-slot Photonic crystal nanocavity	510	2.6×10^4	10^{-5}
[37]	RI biosensor formed by two Waveguide and one microcavity (Double-Hole Defect)	500	1.7 890 10^4	0.0001
This work	Photonic crystal waveguide utilizing width modulated microcavity	539	1.773510^5	10^{-5}

Figure 8a shows the sensitivity and the resonant wavelength variations according to the change of the inner radius (R_{in}) from 0.255a to 0372a and the Figure 8b shows the quality factor as a function of R_{in},which enlarges as the inner ring radius (R_{in}) from 0.256a to 0.372a and reaches its maximum of

$6.388x10^5$ at the resonant mode located at 1.47425nm for R_{in}=0.302a,then followed by a sharp decrease. The increase in the inner radius value is goes along with the decrease of the annular air area. When the R_{in}reaches a value that is more than 0.302athe rings area becomes seriously thin. This results in a reduction in the light confinement within the cavity area and a significant performance of the optical leakages, which have a negative effect on the photon lifetime within the cavity area that results in a sharp decrease in the Q factor value.

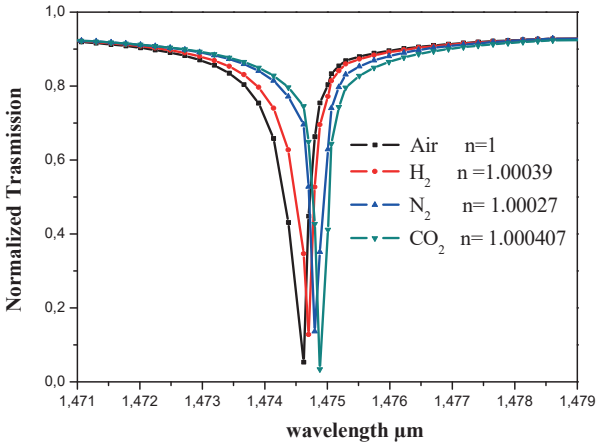

Figure 9. Resonant wavelength changes of the designed sensor as function as a function of changes in the refractive index corresponding to the three infiltration states of gas.

To assess the sensing potential of the sensor, we expose the sample to the gases of different refractive indices, such as, He (1.000139), N_2 (1.000270), and CO_2 (1.000407) [31-33]. The refractive index values were obtained in an atmospheric pressure and were recalculated for λ=1570 nm in room temperature T=20° C using the ideal gas model [35]. The FDTD simulation result show that the resonance wavelength shifts upped by the change of the gas refractive index (figure9).

4. Conclusion

In summary, we have simulated an ultra-compact RI sensor based on tapered-shift defect microcavity introduced to the center of waveguides in the 2D triangular lattice of air holes. A 5.225 nm resonance wavelength shift was observed corresponding to a sensitivity of522.5 nm/RIU for a change in RI value of 0.01.The high-enough sensitivity makes this design useful for realizing photonic crystal-based refractometric and biochemical sensors. And because of the minimized size of the proposed RI sensor, it can be used for measurement in some harsh environments and exceptional conditions.

Acknowledgments

This work is part of the PRFU project No. A25N01UN280120180001 fully funded by the Algerian Ministry of Higher Education and Scientific Research and La Direction Générale de la Recherche Scientifique et du Développement Technologique (DGRSDT).

References

[1] Fan X, White I M, Shopova S I, Zhu H, Suter J D and Sun Y 2008 *Anal. Chim. Acta* **620** 8
[2] Säynätjoki A, Mulot M, Vynck K, Cassagne D, Ahopelto J and Lipsanen H 2008 *Photonics Nanostruct. -Fundam Appl.* **6** 42
[3] Lopez-Torres D, Elosua C, Villatoro J, Zubia J, Rothhardt M, Schuster K and Arregui F J 2017 *Sensor. Actuat. B-Chem.* **251** 1059

[4] Hocini A and Harhouz A 2016 *J. Nanophotonics* **10** 016007
[5] Xu H, Wu P, Zhu C, Elbaz A and Gu Z Z 2013 *J. Mater. Chem. C* **1** 6087
[6] Islam M I, Ahmed K, Sen S, Chowdhury S, Paul B K, Islam M S, Miah M B and Asaduzzaman S 2017 *Photonic. Sens.* **7** 234
[7] Gouveia C, Jorge P A, Baptista J M and Frazao O 2011 *IEEE Sens. J.* **12**1 7
[8] Harhouz A and Hocini A 2015 *J. Electromagn. Waves. Appl.* **29** 659
[9] Arafa S, Bouchemat M, Bouchemat T, Benmerkhi A and Hocini A 2017 *Opt. Commun.***384** 93
[10] Zamani M and Hocini A2016 *Opt. Mater.* **58** 306
[11] Boufenar R, Bouamar M and Hocini A 2017 *Photonics. Nanostruct.* **24** 47
[12] Johnson SG and Joannopoulos JD 2001*Photonic Crystals: the Road from Theory to Practice* (Kluwer Academic, Norwel, MA, USA: Springer Science & Business Media)
[13] Hocini A, Moukhtari R, Khedrouche D, Kahlouche A and Zamani M 2017 *Opt. Commun.* **384** 111
[14] Akahane Y, Asano T, Song B S and Noda S 2003 *Nature.* **425** 944
[15] Song B S, Noda S, Asano T and Akahane Y2005 *Nat. Mater.* **4** 207
[16] Di Falco A, O'faolain L and Krauss T F 2009 *Appl. phys. Lett.* **94** 063503
[17] Notomi M, Yamada K, Shinya A, Takahashi J, Takahashi C and Yokohama I 2001 *Phys. Rev. Lett.* **87** 253902
[18] Notomi M, Shinya A, Yamada K, Takahashi J I, Takahashi C and Yokohama I 2002 *IEEE. J. Quantum. Electron.* **38** 736
[19] Maache M, Hocini A and Khedrouche D 2017 *Chin.J.Phys.* **55** 2318
[20] Kahlouche A, Hocini A and Khedrouche D 2014 *J. Comput. Electron.* **13** 490
[21] Wang X, Xu Z, Lu N, Zhu J and Jin G 2008 *Opt. Commun.* **281** 1725
[22] Joannopoulos J D, Johnson S G, Winn J N and Meade R D 2008 *Molding the Flow of Light*. (Princeton, NJ, USA: Princeton Univ. Press).
[23] Mandal S and Erickson D 2008 *Opt. Express.* **16** 1623
[24] Huang L, Tian H, Yang D, Zhou J, Liu Q, Zhang P and Ji Y 2014 *Opti. Commun.* **332** 42
[25] Huang L, Tian H, Zhou J, Liu Q, Zhang P and Ji Y *Opt. Commun.* **335** 73
[26] Zhou J, Tian H, Yang D, Liu Q and Ji Y 2014 *Opt. Commun.* **330** 175
[27] Kuramochi E, Notomi M, Mitsugi S, Shinya A, Tanabe T and Watanabe T 2006 *Appl. Phys. Lett.* **88** 041112
[28] Joannoupoulos J D, Meade R D and Winn J N 1995 *Photonic Crystals* (Princeton, NJ, USA: Princeton Univ. Press).
[29] Dutta H S, Goyal A K and Pal S2014*J. Nanophotonics.* **8** 083088
[30] Zouache T, Hocini A, Harhouz A and Mokhtari R 2017 *Acta Phys. Pol. A* **131** 68
[31] Le Thomas N, Houdré R, Kotlyar M V, O'Brien D and Krauss T F 2007 *J. Opt. Soc. Am. B* **24** 2964
[32] Canadian Liquid Air Ltd Division scientifique 1976 *Encyclopédie des Gaz* (Elsevier).
[33] Simmons A C 1978 *Opt. Commun.* **25** 211
[34] Sünner T, Stichel T, Kwon S H, Schlereth T W, Höfling S, Kamp M and Forchel A 2008 *Appl. Phys. Lett.* **92** 261112
[35] Wang X, Lu N, Zhu J and Jin G 2008 *Proc. SPIE.* **6831** 68310D
[36] Jágerská J, Zhang H, Diao Z, Le Thomas N and Houdré R 2010 *Opt. let.* **35** 2523
[37] Shiramin L A, Kheradmand R and Abbasi A 2012 *IEEE. Sens. J.* **13** 1483
[38] Villeneuve P R, Fan S and Joannopoulos J D1996 *Phys. Review B* **54** 7837